



## Molecular phylogenetics and floral evolution of the *Cirrhopetalum* alliance (*Bulbophyllum*, Orchidaceae): Evolutionary transitions and phylogenetic signal variation



Ai-Qun Hu<sup>a,b,c</sup>, Stephan W. Gale<sup>b,\*</sup>, Zhong-Jian Liu<sup>d</sup>, Somran Suddee<sup>e</sup>, Tian-Chuan Hsu<sup>f</sup>, Gunter A. Fischer<sup>b</sup>, Richard M.K. Saunders<sup>a,\*</sup>

<sup>a</sup> Division of Ecology & Biodiversity, School of Biological Sciences, The University of Hong Kong, Pokfulam Road, Hong Kong Special Administrative Region

<sup>b</sup> Kadoorie Farm & Botanic Garden, Lam Kam Road, Tai Po, New Territories, Hong Kong Special Administrative Region

<sup>c</sup> Biodiversity Research Center, Academia Sinica, Nankang, Taipei 11529, Taiwan<sup>1</sup>

<sup>d</sup> Key Laboratory of National Forestry and Grassland Administration for Orchid Conservation and Utilization at College of Landscape Architecture, Fujian Agriculture and Forestry University, Fuzhou 350002, China

<sup>e</sup> Forest Herbarium, Department of National Parks, Wildlife and Plant Conservation, Chatuchak, Bangkok 10900, Thailand

<sup>f</sup> Botanic Garden Division, Taiwan Forest Research Institute, No. 53, Nanhai Road, Taipei 10066, Taiwan

### ARTICLE INFO

#### Keywords:

*Bulbophyllum*  
*Cirrhopetalum* alliance  
 Evolutionary transition  
 Monophyly  
 Phylogenetic signal  
 Sect. *Desmosanthes*

### ABSTRACT

The *Cirrhopetalum* alliance is a loosely circumscribed species-rich group within the mega-diverse genus *Bulbophyllum* (Orchidaceae). The monophyletic status of the alliance has been challenged by previous studies, although established sectional classifications have yet to be tested in a phylogenetic context. We used maximum likelihood and Bayesian analyses of DNA sequence data (cpDNA: *matK* and *psbA-trnH*; nrDNA: ITS and *Xdh*; 3509 aligned characters; 117 taxa), including all sections putatively associated with the *Cirrhopetalum* alliance, to reconstruct the phylogeny. We mapped 11 selected categorical floral characters onto the phylogeny to identify synapomorphies and assess potential evolutionary transitions across major clades. Our results unequivocally support the recognition of an amended *Cirrhopetalum* alliance as a well-supported monophyletic group characterized by clear synapomorphies, following the inclusion of sect. *Desmosanthes* and the exclusion of five putative *Cirrhopetalum*-allied sections. Most sections within the *Cirrhopetalum* alliance are demonstrated to be polyphyletic or paraphyletic, necessitating a new sectional classification. The inclusion of sect. *Desmosanthes* revolutionizes our understanding of the alliance, with significant evolutionary transitions in floral characters detected. We further investigated six continuously variable characters of the sepals and labellum, and detect phylogenetic conservatism in labellum width and the evolutionary lability of lateral sepal length, which can partly be explained by the different functional roles they play in pollination and pollinator trapping.

### 1. Introduction

*Bulbophyllum* Thouars—the most species-rich orchid genus with 1900–2200 currently accepted species—represents significant epiphytic diversity in the tropical rainforest canopy (Pridgeon et al., 2014; Chase et al., 2015) and is an excellent model system for elucidating the biological diversity of orchids (Gravendeel et al., 2004; Gamisch and Comes, 2019). *Bulbophyllum* species are characterized by a predominantly epiphytic or lithophytic growth form, with a creeping rhizome that bears a series of 1- or 2-leaved pseudobulbs (very rarely absent) and their flowers commonly feature a fleshy and mobile ligulate

labellum and morphologically diverse lateral sepals that vary in size, shape, color and surface ornamentation. *Bulbophyllum* has had a complex taxonomic history: since its establishment (Thouars, 1822), taxonomists have described at least two dozen closely allied genera, mostly distinguished based on floral morphology (summarized by Seidenfaden, 1979; Pridgeon et al., 2014); all these genera, however, have subsequently been combined within a broader circumscription of *Bulbophyllum* that has been recognized as monophyletic in recent molecular studies (Gravendeel et al., 2014; Chase et al., 2015). The size and ambiguous infrageneric systematics of this unwieldy genus has generated considerable difficulty, impeding studies of floral evolution,

\* Corresponding authors.

E-mail addresses: [stephangale@kfbg.org](mailto:stephangale@kfbg.org) (S.W. Gale), [saunder@hku.hk](mailto:saunder@hku.hk) (R.M.K. Saunders).

<sup>1</sup> Present address.

ecology and morphology that would have benefitted from the recognition of narrower taxonomic groupings. Our knowledge is furthermore regionally limited, with a significant gap in tropical Asia, which is an important center of diversity for the genus, with c. 1500 accepted species. While complete taxon sampling of such a large genus throughout its range is an unrealistic challenge, our present study—which focuses on the predominantly Asian *Cirrhopetalum* alliance—undoubtedly represents a major step towards a more comprehensive reassessment of the systematics of *Bulbophyllum*.

The loosely circumscribed ‘*Cirrhopetalum* alliance’ is an association of sections derived from *Cirrhopetalum* Lindl., which was previously regarded as a genus separate from *Bulbophyllum*. Species of the *Cirrhopetalum* alliance can be recognized by their subumbellate inflorescences and/or flowers generally with fringed sepals/petals and significantly elongated lateral sepals that are twisted and connate for at least part of their length (Holttum, 1957; Seidenfaden, 1973). Seidenfaden (1973) listed more than 240 species (assigned to five groups equivalent to sections) in the *Cirrhopetalum* alliance, distributed in Africa (c. 3 species), Madagascar (1 species), northern Australia (c. 3 species) and Asia (the center of diversity, with c. 233 species). The complex systematics of the *Cirrhopetalum* alliance significantly impedes research. The homogeneous morphology of vegetative characters and homoplastic flowers, even between distantly related *Cirrhopetalum* species, renders sectional taxonomy problematic, even for specialists. Following Seidenfaden’s (1973) research, two contrasting classifications of the *Cirrhopetalum* alliance were proposed (summarized in Table 1), firstly by Garay et al. (1994) and subsequently in multiple studies by Vermeulen and co-authors (Chen and Vermeulen, 2009; Vermeulen, 2014; Vermeulen et al., 2014, 2015).

None of these classifications are well aligned with the topologies revealed by the currently available phylogenies, although it should be noted that these phylogenetic reconstructions are based on limited molecular data. The study by Gravendeel et al. (2014), for example, was based on a single nuclear DNA region (the internal transcribed spacer, ITS), but suggested that the ‘core’ *Cirrhopetalum* alliance (including species of sect. *Recurvae* Garay et al. and sect. *Cirrhopetalum*) was sister to sect. *Racemosae* Benth. & Hook.f., while two sections putatively associated with the *Cirrhopetalum* alliance, viz. *Lemniscata* Pfitzer and *Reptantia* J.J. Verm. ex N. Pearce et al., formed a clade that was phylogenetically distant from the core clade. Although these preliminary results indicate that the *Cirrhopetalum* alliance as previously circumscribed might not be monophyletic, the phylogeny lacks statistical support and is based on inadequate taxon sampling. A more recent study by Wang et al. (2017), based on both nuclear and chloroplast DNA sequences of 19 species of the *Cirrhopetalum* alliance (c. 11%), also indicated a well-supported ‘core’ *Cirrhopetalum* framework. It was further revealed that three included sections, *Brachyantha* Rchb.f., *Cirrhopetalum* and *Cirrhopetaloides* Garay et al., were retrieved as polyphyletic or paraphyletic with equivocal support.

In another study, Hosseini et al. (2016) retrieved an ambiguous relationship between the *Cirrhopetalum* alliance and sect. *Desmosanthes*

(Blume) J.J. Smith, based on combined nuclear and chloroplast DNA sequences of 12 species (c. 7%) from the alliance: sect. *Desmosanthes* is nested inside the *Cirrhopetalum* alliance, rendering both lineages either polyphyletic or paraphyletic. This result further challenges the monophyly of the *Cirrhopetalum* alliance, suggesting that the alliance should possibly be expanded to include sect. *Desmosanthes*. Hosseini et al. (2016) further investigated six characters to identify putative synapomorphy and concluded that sect. *Cirrhopetalum* can be characterized by an umbellate inflorescence, lateral sepals that are longer than the dorsal sepal, and fringed margins of the petals and dorsal sepal, hence partly corroborating the opinions of Holttum (1957) and Seidenfaden (1973). Hosseini et al. (2016) distinguished sect. *Desmosanthes* from the *Cirrhopetalum* alliance based on its non-fringed petals and dorsal sepal. The scenario in which the *Cirrhopetalum* alliance is expanded to include morphologically heterogeneous components from sect. *Desmosanthes* suggests that significant evolutionary transitions in floral morphology occurred in the *Cirrhopetalum* alliance. However, these hypotheses are yet to be tested.

Phylogenetic signal can be defined as the evolutionary trend for closely related species to resemble each other more closely (in terms of life history traits) than other species randomly drawn from the phylogeny (Blomberg and Garland, 2002; Blomberg et al., 2003). High phylogenetic signal in a trait is often interpreted as evolutionary or phylogenetic conservatism (Losos, 2008) due to stabilizing selection, limited genetic variation, low rates of evolution, physiological constraints or various biotic interactions (such as competition), hence restricting the evolution of new phenotypes (Blomberg and Garland, 2002; Wiens et al., 2010; de Mazancourt et al., 2008; Bradshaw, 1991). Conversely, low phylogenetic signal is often inferred as the trait being evolutionarily labile (Blomberg et al., 2003) or due to high rates of trait evolution leading to significant divergence among close relatives. Considerable variation in terms of floral form, shape, size and color are observed and recorded in the *Cirrhopetalum* alliance (Fig. 1), although the evolutionary patterns have rarely been tested in a phylogenetic context. In the present study, we assess phylogenetic signal for selected floral traits in the *Cirrhopetalum* alliance (six size measurements from the dorsal sepal, lateral sepals and labellum) that perform different roles during pollinator trapping (Christensen, 1994; van der Cingel, 2001). This trapping mechanism functions with the mobile labellum acting as a ‘see-saw’ that traps the pollinator by physically forcing it against the column, thereby depositing or retrieving pollinia, whilst the lateral sepals serve as the primary landing platform, directing the pollinator to access the labellum; olfactory and visual attractants furthermore prolong visits, promote interfloral movement and increase the probability of pollen transfer when pollinator service is limiting, as is usually the case with deception pollination systems (Jersáková et al., 2006; Scopece et al., 2010). Pollinators occasionally also land on the dorsal sepal, which is almost uniformly hood-shaped and functionally more likely to provide protection to the column against rain. We have observed that although lateral sepals exhibit tremendous diversity in arrangement, shape, size and color (Fig. 1), the labellum is nevertheless

**Table 1**  
Comparison of representative sectional classifications of the *Cirrhopetalum* alliance.

Author	Genus	Section (accepted species)
Garay et al. (1994)	<i>Bulbophyllum</i> Thouars	<i>Biflorae</i> Garay et al., <i>Cirrhopetaloides</i> Garay et al., <i>Elatae</i> Garay et al., <i>Emarginatae</i> Garay et al., <i>Macrostylidia</i> Garay et al., <i>Medusa</i> Garay et al., <i>Microbulbon</i> Garay et al., <i>Pahudiella</i> Garay et al., and <i>Umbellatae</i> Benth. & Hook.f. (57 spp.)
Chen and Vermeulen (2009), Vermeulen (2014), and Vermeulen et al. (2014, 2015)	<i>Cirrhopetalum</i> Lindl. <i>Mastigion</i> Garay et al. <i>Rhytionanthos</i> Garay et al. <i>Bulbophyllum</i>	<i>Cirrhopetalum</i> (Lindl.) P. Royen, <i>Recurvae</i> Garay et al., and <i>Wallichii</i> Garay et al. (98 spp.) (5 spp.) (10 spp.) <i>Biflorae</i> , <i>Blepharistes</i> J.J. Verm. et al., <i>Brachyantha</i> Rchb.f., <i>Cirrhopetaloides</i> Garay et al., <i>Cirrhopetalum</i> (Lindl.) P. Royen, <i>Emarginatae</i> Garay et al., <i>Ephippium</i> Schltr., <i>Eublepharon</i> J.J. Verm. et al., <i>Lemniscata</i> Pfitzer, <i>Macrostylidia</i> , <i>Plumata</i> J.J. Verm. et al., <i>Reptantia</i> J.J. Verm. ex N. Pearce et al., and <i>Rhytionanthos</i> (Garay et al.) J.J. Verm. et al. (c.180 spp.)

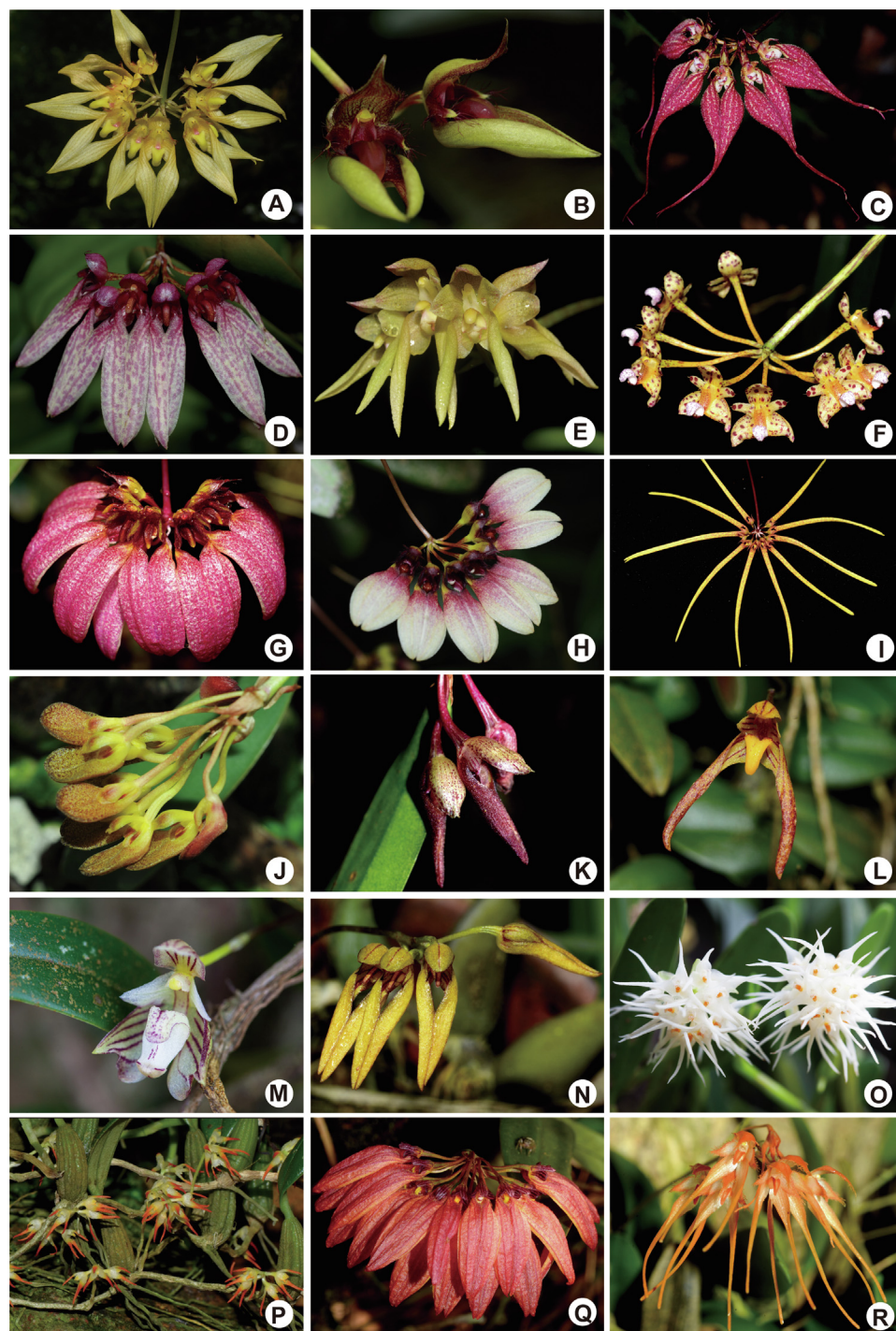


**Fig. 1.** Diversity in floral morphology across major clades/subclades retrieved within the *Cirrhopetalum* alliance. A *Bulbophyllum annandalei* (Clade A); B *B. frostii* (Clade A), with pouch-shaped lateral sepals; C *B. rothschildianum* (Clade A), with motile appendages on the margins of dorsal sepals and petals; D *B. longiflorum* (Clade B), type species of the previously recognized genus *Cirrhopetalum* Lindl.; E *B. umbellatum* (Clade B), with lateral sepal upper margins basally twisted, but not connate; F *B. violaceolabellum* (Clade B), with lateral sepals that are similar in length to the dorsal sepal; G *B. auratum* (Clade C); H *B. lepidum* (Clade C); I *B. makoyanum* (Clade C), with flowers symmetrically arranged; J *B. spathulatum* (Subclade D1); K *B. unciniferum* (Subclade D1), with horn-shaped lateral sepals; L *B. tipula* (Subclade D2), with a single-flowered inflorescence and free lateral sepals; M *B. ambrosia* (Subclade D3), with a single-flowered inflorescence and an enlarged labellum; N *B. helena* (Subclade D4), with horn-shaped lateral sepals; O *B. odoratissimum* (Subclade D4), with compressed racemose inflorescences; P *B. stenobulbon* (Subclade D4), with compressed racemose inflorescences; Q *B. retusiusculum* (Subclade D5); R *B. taiwanense* (Subclade D7). Species shown in A, C, D, G, H and Q exhibit ‘typical *Cirrhopetalum*’ traits, namely a subumbellate inflorescence and elongated lateral sepals that are basally twisted and with connate upper margins; clades/subclades designations correspond to those shown in Fig. 2.) – Photographs: C, J.W. Li; all others, A.Q. Hu.

relatively conserved (invariably tongue-shaped and of moderate size). We therefore hypothesize that there is considerable phylogenetic signal variation among floral traits linked to functions associated with pollination in the *Cirrhopetalum* alliance.

Previous phylogenetic studies (Gravendeel et al., 2014; Hosseini et al., 2016; Wang et al., 2017) have highlighted several key questions and hypotheses that are yet to be tested. Taxon sampling and phylogenetic resolution and support in these previous studies were inadequate for achieving robust assessments of monophyly, and hence relationships or patterns of floral evolution in the *Cirrhopetalum* alliance remain elusive. The present study addresses these shortcomings by reconstructing the phylogeny of the *Cirrhopetalum* alliance using a greatly extended taxon sampling (97 accessions of 95 species) that includes

representatives of all *Cirrhopetalum*-allied sections, and a significantly expanded dataset based on two chloroplast regions (*matK* and *psbA-trnH*) and two nuclear regions (ITS and *Xdh*). We aim to: (1) assess the putative monophyly of the *Cirrhopetalum* alliance and identify elements that should possibly be excluded or included; (2) identify synapomorphies and evolutionary transitions in floral characters among major clades; and (3) elucidate variation in phylogenetic signal between the sepals and labellum.

## 2. Materials and methods

### 2.1. Taxon sampling

We included 119 accessions, representing 117 species, in our phylogenetic analyses (Supplementary Table S1). Five species of *Dendrobium* Sw. were selected as the outgroup (with sequences downloaded from GenBank; Supplementary Table S1) since *Dendrobium* has consistently been retrieved as sister to *Bulbophyllum* within subtribe Dendrobiinae (Xiang et al., 2013; Pridgeon et al., 2014; Chase et al., 2015). The remaining 114 accessions (112 species) of *Bulbophyllum* represent sects. *Acrochaene* (Lindl.) J.J. Verm et al. (1 sp.), *Biseta* J.J. Verm. ex N. Pearce et al. (1 sp.), *Monomeria* (Lindl.) J.J. Verm et al. (1 sp.), *Leopardinae* Benth. (5 spp.), *Racemosae* (4 spp.), *Sestochilos* (Breda) Benth. & Hook.f. (2 spp.), *Stenochilus* J.J. Sm. (1 sp.), *Ione* (Lindl.) J.J. Verm et al. (2 spp.), and a broad representation of putative lineages within the *Cirrhopetalum* alliance. Sampling of the alliance itself included 97 accessions (95 species), representing all putatively associated sections, viz.: *Biflorae* Garay et al., *Blepharistes* J.J. Verm et al., *Brachyantha*, *Cirrhopetaloides*, *Cirrhopetalum*, *Desmosanthes*, *Emarginatae* Garay et al., *Ephippium* Schltr., *Eublepharon* J.J. Verm et al., *Lemniscata*, *Macrostylidia* Garay et al., *Medusa*, *Plumata* J.J. Verm et al., *Reptantia*, and *Rhytionanthos* Garay et al.

### 2.2. DNA extraction and sequencing

Total genomic DNA was extracted from silica-dried or fresh leaf material using the DNeasy plant mini kit (QIAGEN, Hong Kong) following the manufacturer's instructions. A modified CTAB method (Doyle and Doyle, 1987), combined with the DNeasy plant mini kit, was used for leaf material that was rich in secondary metabolites and polysaccharides. Four DNA regions were selected for sequencing based on their informative quality evidenced in previous family-wide (see review in Chase et al., 2015) or *Bulbophyllum*-focused phylogenetic studies (Fischer et al., 2007; Smidt et al., 2011; Hosseini et al., 2012, 2016): two chloroplast regions (*matK* and *trnH-psbA*) and two nuclear regions (ITS and *Xdh*). Information on primers and PCRs conditions is provided in Supplementary Table S2. Raw sequences were edited using Geneious ver. 8.1.7 (Kearse et al., 2012). Sequences of each individual region were aligned using the default settings in the Geneious plugin MAFFT (Katoh et al., 2009) and adjusted manually. A total of 423 new sequences were generated in this study, with Genbank accessions listed in Table S1.

### 2.3. Phylogenetic analyses

The two chloroplast regions were concatenated, resulting in a matrix of 2014 base pairs (hereafter referred to as the 'cpDNA dataset'), as were the two nuclear regions, forming a matrix of 1494 base pairs (the 'nrDNA dataset'). These two datasets were used to run maximum likelihood (ML) and two independent Bayesian inference (BI) phylogenetic analyses to test for possible topological incongruence. The best evolutionary model was estimated prior to phylogenetic reconstruction using jModelTest 2 (Darriba et al., 2012): the GTR + I + G model was identified as best for both datasets. Models were implemented in the ML analysis with RAxML-HPC2 Workflow (Stamatakis, 2014) on the CIPRES Science Gateway ver. 3.3 (Miller et al., 2010). The ML/Thorough bootstrap workflow was followed by searching for the best-scoring ML tree and then calculating branch support values with RaxML by halting bootstrapping automatically under the autoMRE criterion. One hundred references were run from a distinct randomized maximum parsimony starting tree with other parameters set to default.

BI was conducted using MrBayes ver. 3.2.6 (Huelskenbeck and Ronquist, 2001) on CIPRES. In each analysis, four simultaneous Markov chain Monte Carlo (MCMC) chains (containing three heated chains and one cold chain with a temperature parameter of 0.16) were run for 20

million generations. To avoid problems posed by the extremely long trees highlighted in previous studies (Brown et al., 2010; Marshall, 2010), the default command 'brlenspr = unconstrained: gammadir (1, 0.1, 1, 1)' was used (Zhang et al., 2012). Visual comparison of phylogenies derived from the separate analysis of the datasets did not identify topological incongruence (see Figs. S1, S2), and hence cpDNA and nrDNA matrices were concatenated, resulting in a final matrix of 3509 base pairs (hereafter referred to as the 'combined dataset'). Both ML and BI analyses were conducted on the combined dataset with similar parameters as applied above. Convergence of independent runs was examined with the R package AWTY (Nylander et al., 2008) and assessed by checking that the standard deviation of split frequencies was  $< 0.005$ . Adequate effective sample sizes (ESS  $> 200$ ) were verified using Tracer ver.1.6 (Rambaut et al., 2014). Outputs of all phylogenetic analyses were read using Figtree ver. 1.4.2 (Rambaut, 2014).

To obtain ultrametric trees suitable for comparative methods, we estimated the 119-accession data matrix extended following the addition of six further outgroup species from *Dendrobium* (Table S1), with the Bayesian relaxed molecular clock model with uncorrelated log-normal rates in BEAST ver. 2.4.4 (Bouckaert et al., 2014). The birth-death prior on node ages was selected against the Yule prior after model testing by Bayes factors (BF  $> 100$ ) based on preliminary runs as implemented in Tracer. Two secondary calibrations (one for the *Dendrobium* clade and the other for the *Bulbophyllum*-*Dendrobium* clade) were applied in this study based on previous analyses (Conran et al., 2009; Gamisch et al., 2015). We conducted five independent MCMC runs of 50 million generations with sampling every 5000 generations. After evaluating convergence with the R package AWTY and effective sample sizes in Tracer (ESS  $> 200$ ), we combined the five independent runs with LogCombiner ver. 2.1.3 (Rambaut and Drummond, 2014), setting the burn-in to 25% of the initial samples of each run. We further used TreeAnnotator ver. 2.1.3 (Bouckaert et al., 2014) to compute the maximum clade credibility (MCC) tree for downstream comparative study.

### 2.4. Character reconstructions and phylogenetic signal in floral traits

In total, 17 floral characters were investigated (Table 3)—11 categorical floral characters were mapped onto the phylogeny to identify putative synapomorphies (inflorescence type, the number of flowers per inflorescence, shape and connation of lateral sepals, and the margin indument of sepals and petals), detect evolutionary transitions (color of sepals and petals, floral scent, and spots/markings/stripes on the sepals/petals/labellum); six continuously variable floral characters in the sepals and labellum (dorsal sepal, lateral sepal and labellum dimensions) were measured to test phylogenetic signal. Coding of the characters is detailed in Table 3, with the taxon-character matrix presented as Supplementary Tables S3 (11 categorical characters) and S4 (six continuously variable characters). Character state data were obtained by scoring living plants (from natural populations or in cultivation), herbarium material (dry and liquid-preserved specimens), or from the published literature (Seidenfaden, 1973, 1979; Vermeulen and Coote, 2008; Chen and Vermeulen, 2009; Barreto et al., 2011; Vermeulen et al., 2014, 2015; Averyanov et al., 2016; Hu et al., 2017a; Zhai et al., 2017).

For the 11 categorical characters, ancestral character state reconstructions were conducted on a 100-accession phylogeny with two independent methods, MP and ML as implemented in Mesquite ver. 2.7.5 (Maddison and Maddison, 2011), to allow for possible incongruence. Character-state changes were set as unordered, with characters traced over the 1000 MCMC trees (selected from the post-burn-in posterior distribution of Bayesian trees based on combined dataset) using default settings in the MP analyses. The ML analyses were performed under the Mk1 evolutionary model (the one-parameter Markov k-state model; Lewis, 2001), specifying that any change of state is of equal probability and incorporating a single parameter. The 'Average

Frequencies across Trees' option was used to estimate the average likelihood of each state at each node across all trees possessing that node. The overall results were summarized on the Bayesian majority rule consensus tree from the combined dataset.

To test the hypothesis of phylogenetic signal variation among floral traits in the *Cirrhopetalum* alliance, two metrics—Pagel's  $\lambda$  (Pagel, 1997, 1999) and Blomberg's  $K$  (Blomberg and Garland, 2002)—were estimated for the six continuous traits (Table 3) using the function 'phylosig' in the R package phytools (Revell, 2012). Analyses were conducted on the topology comprising 88 accessions of the *Cirrhopetalum* alliance (Supplementary Table S4) extracted from the MCC tree. Three different evolutionary models—Brownian motion model (BM), Ornstein-Uhlenbeck model (OU) and White noise model (WH)—were assessed with the function 'fitContinuous' in the R package geiger (Harmon et al., 2008) to determine which model best explains the evolutionary patterns of the traits. The classic BM evolutionary model assumes random walk divergences in species resemblance (Felsenstein, 1973). The OU model is a modification of the BM model with an additional parameter, alpha ( $\alpha$ ), which measures the strength of return towards a theoretical optimum that is shared across a clade or subset of species (Hansen, 1997). The WH model assumes no phylogenetic signal and that the data come from a single normal distribution with no covariance structure among species (Harmon et al., 2008).

Correlations between sepal and labellum traits are expected because they are potentially closely linked to pollination. We specifically focused on two variables—the lateral sepal length (LSL) and labellum width (LW)—which were indicated as having contrasting evolutionary patterns based on the estimated Pagel's  $\lambda$  and  $K$  values (see Results 3.3). To test whether these contrasting patterns can be predicted by the other five putatively associated traits (the predictor variables), we regressed LSL and LW (the response variables) against the values of five individual traits and a combination of five other traits with phylogenetic generalized least squares (PGLS; Martins and Hansen, 1997). The function 'pgls' in the R package caper (Orme et al., 2013) was applied, fitting  $\lambda$  based on ML.

### 3. Results

#### 3.1. Phylogenetic reconstruction

The general statistics of the alignments for individual regions and combined datasets and the best-fit nucleotide substitution models for each region in the BI analyses are summarized in Table 2. Significant incongruence was not detected among the topologies based on the cpDNA and nrDNA datasets (Figs. S1 and S2). The ML and BI analyses based on the combined data matrix resulted in better resolved topologies with higher node support compared to those from the separate cpDNA and nrDNA datasets; these results were therefore summarized on the Bayesian majority rule consensus tree in the following discussion (Fig. 2). Sectional placement of species was added (Fig. 2) according to

**Table 2**

Summary statistics for the four DNA regions and three datasets used in this study.

DNA region	Accessions	Alignment length (base pairs)	Variable characters (percent)	Parsimony-informative characters (percent)
<i>matK</i>	108	1147	236 (20.6%)	156 (13.6%)
<i>psbA-trnH</i>	104	887	163 (18.4%)	65 (7.3%)
ITS	116	774	422 (54.5%)	323 (41.2%)
<i>Xdh</i>	109	727	258 (35.5%)	138 (19.0%)
cpDNA	114	2014	417 (20.7%)	238 (11.8%)
nrDNA	119	1496	684 (45.7%)	465 (31.1%)
Combined dataset	119	3509	1094 (31.2%)	705 (20.1%)

Chen and Vermeulen (2009), Vermeulen (2014) and Vermeulen et al. (2014, 2015), supplemented by more recent species descriptions and amended sectional placements (Averyanov et al., 2016; Hu et al., 2017a; Zhai et al., 2017).

The core *Cirrhopetalum* alliance clade (CAC) was strongly supported (PP = 1; BP = 85) as monophyletic following the exclusion of five putatively associated sections (*Biflorae*, *Biseta*, *Blepharistes*, *Lemniscata* and *Reptantia*) and the inclusion of a previous outlier, sect. *Desmosanthes*, which was found to be nested within the alliance. Sect. *Leopardinae* was strongly supported as sister to the CAC in BI (PP = 0.98), but only weakly supported in ML (BP = 53).

Four major clades (labelled A–D in Fig. 2) are recognized within the CAC, each with strong to moderate support: Clade A (PP = 1; BP = 87); Clade B (PP = 1; BP = 100); Clade C (PP = 1; BP = 100); and Clade D (PP = 0.99; BP = 78). Clade D was furthermore subdivided into seven subclades (D1–D7). Relationships among the four major clades were nevertheless poorly resolved. Several of these clades or subclades broadly correspond with taxa elucidated in previous classifications of the *Cirrhopetalum* alliance, but the majority of existing sections were not retrieved as monophyletic.

#### 3.2. Ancestral character state reconstructions

The parsimony and likelihood ancestral floral trait reconstructions of the 11 categorical characters are presented in Figs. 3–5 and Supplementary Figs. S3–S10.

Subumbellate inflorescences (Character 1; Fig. 3) and lateral sepals that are basally twisted (Character 3; Fig. 4) with their upper margins connate (Character 4; Fig. 5) are identified as synapomorphies for the CAC. However, departure from this combination of synapomorphies is observed in Subclades D3 and D4: species in these clades possess flowers with sepals that are similar in shape and size, with free lateral sepals that are neither twisted nor fused; and species in clade D4 possess racemose inflorescences. Our results furthermore suggest a suite of plesiomorphic states for the CAC, including inflorescences comprising multiple pigmented flowers (Characters 2 and 6; Supplementary Figs. S3 and S4) without any perceptible floral scent (Character 6; Supplementary Fig. S5), dorsal sepal/petals with glabrous margins (Characters 7 and 8; Supplementary Figs. S6 and S7), and spotted or marked sepals/petals/labellum (Characters 9 and 10; Supplementary Figs. S8 and S9). A labile evolutionary pattern was detected with respect to stripes on the sepals and petals (Character 11; Supplementary Fig. S10). Selected characters are discussed in detail below.

Arrangement of lateral sepals (Characters 3 and 4; Figs. 4 and 5): unlike most CAC species, in which the lateral sepals are twisted and connate, those in Subclades D3 and D4 are not twisted and are free along their upper margins. Transitions to straight, free lateral sepals are rare (mainly occurring in Subclades D3 and D4).

Number of flowers per inflorescence (Character 2; Supplementary Fig. S3): inflorescences with multiple flowers are reconstructed as plesiomorphic for the CAC, with transitions to single-flowered (rarely 2–3-flowered) inflorescences occurring independently at least six times during the diversification of the CAC.

Floral scent (Character 6; Supplementary Fig. S5): an imperceptible floral odor is retrieved as plesiomorphic for the CAC. The transition to a scent that is reminiscent of decaying organic matter occurs in Clade A. This character state is also exhibited by several species in Clade B and Subclade D4, although the ancestral states for relevant nodes are equivocal. Fruity scents are also revealed as derived, exhibited in many lineages within Subclade D4. At least six similar independent transitions are observed in other clades (B, C, D3 and D5).

Dorsal sepal/petal margin indument (Characters 7 and 8; Supplementary Figs. S6 and S7): the presence of hairs on the margins of the dorsal sepal and petals is likely to be linked as the ancestral character state reconstructions reveal a similar pattern for both. A transition from glabrous (plesiomorphic for the CAC) to hairy dorsal sepal/petal

**Table 3**

List of 17 floral characters (11 categorical and six continuous) used in the character state analysis.

Code	Character	Coding
Character 1	Inflorescence type	0 = ambiguous (i.e. 1-flowered, or rarely 2–3-flowered); 1 = subumbellate; 2 = racemose (either compressed or elongated);
Character 2	Number of flowers per inflorescence	0 = 1–3; 1 = > 3;
Character 3	Lateral sepal shape	0 = basally twisted; 1 = not basally twisted;
Character 4	Lateral sepal margin connation	0 = upper margins connate; 1 = lower margins connate; 2 = free;
Character 5	Sepal and petal color	0 = white or yellowish; 1 = other colors;
Character 6	Floral scent	0 = reminiscent of decaying organic matter; 1 = fruity; 2 = imperceptible
Character 7	Dorsal sepal margin indument	0 = glabrous; 1 = hairy;
Character 8	Petal margin indument	0 = glabrous; 1 = hairy;
Character 9	Spots/markings on sepals and petals	0 = present; 1 = absent;
Character 10	Spots/markings on labellum	0 = present; 1 = absent;
Character 11	Stripes on sepals and petals	0 = present; 1 = absent;
Character 12	Mean dorsal sepal length (DSL)	Continuous (mm)
Character 13	Mean dorsal sepal width (DSW)	Continuous (mm)
Character 14	Mean lateral sepal length (LSL)	Continuous (mm)
Character 15	Mean lateral sepal width (LSW)	Continuous (mm)
Character 16	Mean labellum length (LL)	Continuous (mm)
Character 17	Mean labellum width (LW)	Continuous (mm)

margins occurred in clades A, B, C, D6 and D7.

### 3.3. Phylogenetic signal and floral trait correlations

The six continuously variable characters tested in the present study are all shown to possess significant phylogenetic signal according to Pagel's  $\lambda$  (significantly different from 0;  $P$ -value < 0.01) and K statistics (significantly different from 1;  $P$ -value < 0.01) based on both absolute and log-transformed variables (Table 4). Pagel's  $\lambda$  ranged from 0.72–0.97 (absolute values) and 0.82–0.96 (log-transformed values); whilst K ranged from 0.45–1.28 (absolute values) and 0.65–1.15 (log-transformed values). Notice that the Pagel's  $\lambda$  values are significantly different from 1 in five of the six continuous characters based on log-transformed variables ( $P$ -value < 0.01), indicating that although there is considerable phylogenetic signal, other evolutionary processes might be playing a role rather than the pure Brownian motion in these traits. Fitting three different evolutionary models to the data further revealed that the assumption of no phylogenetic signal in traits under the WH model is invariably rejected (OU ~ WH:  $pchisq < 0.05$ ; Table 4); the OU model is favored over BM and better explains the evolutionary trend of DSW, LL and LW (OU ~ BM:  $pchisq < 0.05$ ). Under the OU model, the  $\alpha$  values that describe the strength of pull towards a central value (typically referred to as the trait or selective optima) are relatively low in DSW, LL and LW (0.96, 0.75 and 0.78, respectively). The rate of character evolution ( $Sig^2$ ) under BM model ranged from 0.006 to 0.021, with the highest in LSL and lowest in DSL (Table 4).

PGLS analyses indicated a moderate correlation between four traits and LW (Table 5), with adjusted  $R^2$  ranging from 0.16 to 0.58. Overall, 81% of the variance found in LW can be explained by the combination of the other five variables. Conversely, a relatively weak correlation was demonstrated between LSL and most individual traits, with  $R^2$  ranging from 0.03 (against LW) to 0.18 (against DSL) and the combination of the other five variables only reflecting 18% of LSL variance. Remarkably, there was no correlation between LSL and LW with  $P > 0.05$  for models LSL ~ LW and LW ~ LSL, respectively.

## 4. Discussion

### 4.1. Monophyly and floral transitions of the amended *Cirrhopetalum* alliance

The robust phylogenetic framework presented here demonstrates that the *Cirrhopetalum* alliance can be maintained as a recognized, monophyletic taxon following the exclusion of five sections that have previously been associated with the alliance—viz. *Biflora*, *Biseta*,

*Blepharistes*, *Lemniscata* and *Reptantia* (Seidenfaden, 1973, 1979)—and the inclusion of a previous outlier, sect. *Desmosanthes* (Fig. 2). The amended *Cirrhopetalum* alliance is demonstrated to be sister to sect. *Leopardinae*, with no evidence to support a sister relationship with sect. *Racemosae* as inferred by Gravendeel et al. (2014).

Strikingly, sect. *Desmosanthes* is unequivocally shown to be nested within the CAC, contradicting the sister relationship proposed by Hosseini et al. (2016). The inclusion of sect. *Desmosanthes*, which comprises c. 65 currently accepted species (Vermeulen, 2014; Vermeulen et al., 2015), requires the expansion of the *Cirrhopetalum* alliance to c. 210 species. Although the inclusion of sect. *Desmonanthes* in the *Cirrhopetalum* alliance has never previously been proposed, it has been noted that establishing a clear dividing line between the two lineages is problematic (Seidenfaden, 1979). A distinction based solely on a comparison of the length of the lateral sepals relative to that of the dorsal sepal is indeed highly artificial and has resulted considerable taxonomic confusion (Seidenfaden, 1973, 1979; Vermeulen et al., 2015). For example, *Bulbophyllum medusae* (Lindl.) Rchb.f., a taxonomically controversial species, has frequently been transferred between sect. *Desmosanthes* and the *Cirrhopetalum* alliance (e.g. Holtum, 1964; Seidenfaden, 1973; Seidenfaden and Wood, 1992; Vermeulen et al., 2015). Since the species formerly accommodated in sect. *Desmosanthes* now account for almost one-third of species diversity in the expanded *Cirrhopetalum* alliance, the newly included species clearly represent an important and previously unrecognized component of the alliance.

The expanded *Cirrhopetalum* alliance is nevertheless well supported by a suite of morphological synapomorphies (Figs. 3–5), viz. a subumbellate inflorescence and lateral sepals with upper margins that are basally twisted and connate with each other. Although these character states are of considerable diagnostic value for recognizing the *Cirrhopetalum* alliance, attention should nevertheless be directed toward the significant transitions in floral morphologies evident within Subclades D3 and D4 (Figs. 3–5). Subclade D3 is represented by a single species, *B. ambrosia* (Hance) Schltr. (Fig. 1M), while Subclade D4 mainly includes species from sect. *Desmosanthes* (the DES group) that are characterized by racemose inflorescences (either compressed or elongated), and flowers with free lateral sepals that are not significantly differentiated in shape and size from the dorsal sepal (e.g. Fig. 1O, P; Vermeulen et al., 2015). The floral transitions identified among the different clades of the *Cirrhopetalum* alliance could be associated with pollinator shifts, a hypothesis which deserves greater attention in future studies that integrate phylogenetics with the pollination biology of species representative of the major clades.

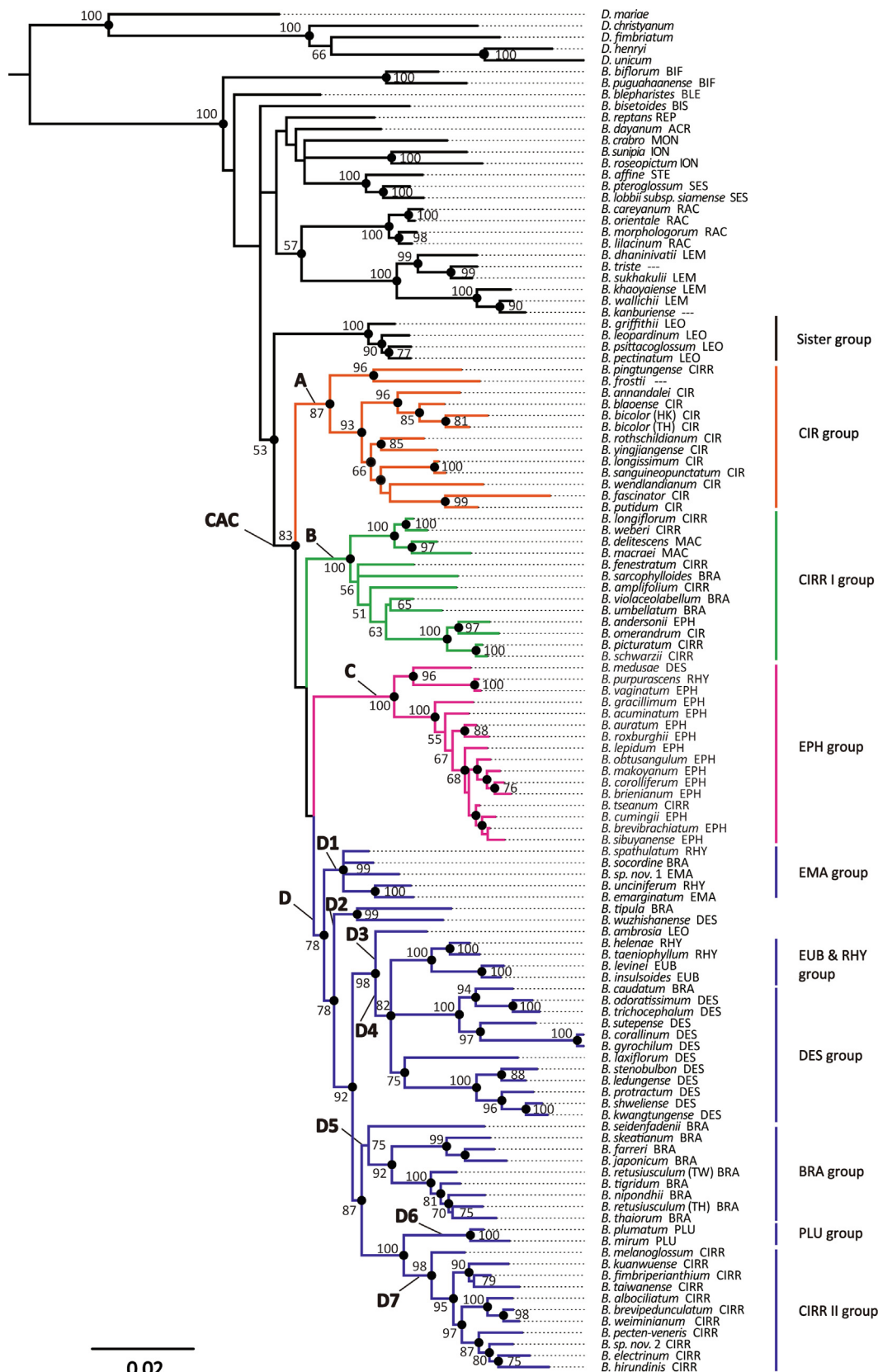


**Fig. 2.** Bayesian majority rule consensus tree resulting from analysis of the combined dataset. Black dots indicate clades receiving posterior probabilities (PP) > 0.95. ML bootstrap support values (BP) > 50 are shown above branches. The four major clades (A–D) and seven subclades (D1–D7) of the *Cirrhopetalum* alliance clade (CAC) are indicated. *B.* = *Bulbophyllum*, *D.* = *Dendrobium*. Sectional placement of taxa (according to the literature cited in Section 3.1) is indicated by 3- or 4-letter abbreviations following the taxon name: ACR: *Acrochaena*, BIF: *Biflorae*, BIS: *Biseta*, BLE: *Blepharistes*, BRA: *Brachyantha*, CIR: *Cirrhopetalum*, DES: *Desmosanthes*, EMA: *Emarginatae*, EPH: *Ephippium*, EUB: *Eublepharon*, ION: *Ione*, LEM: *Lemmiscata*, LEO: *Leopardinae*, MAC: *Macrostylida*, MED: *Medusa*, MON: *Monomeria*, PLU: *Plumata*, RAC: *Racemosae*, REP: *Reptantia*, RHY: *Rhytidanthos*, SES: *Sestochilos*, STE: *Stenochilus*.

## Inflorescence type

- █ Ambiguous
- █ Subumbellate
- █ Racemose
- █ Node absent
- Equivocal

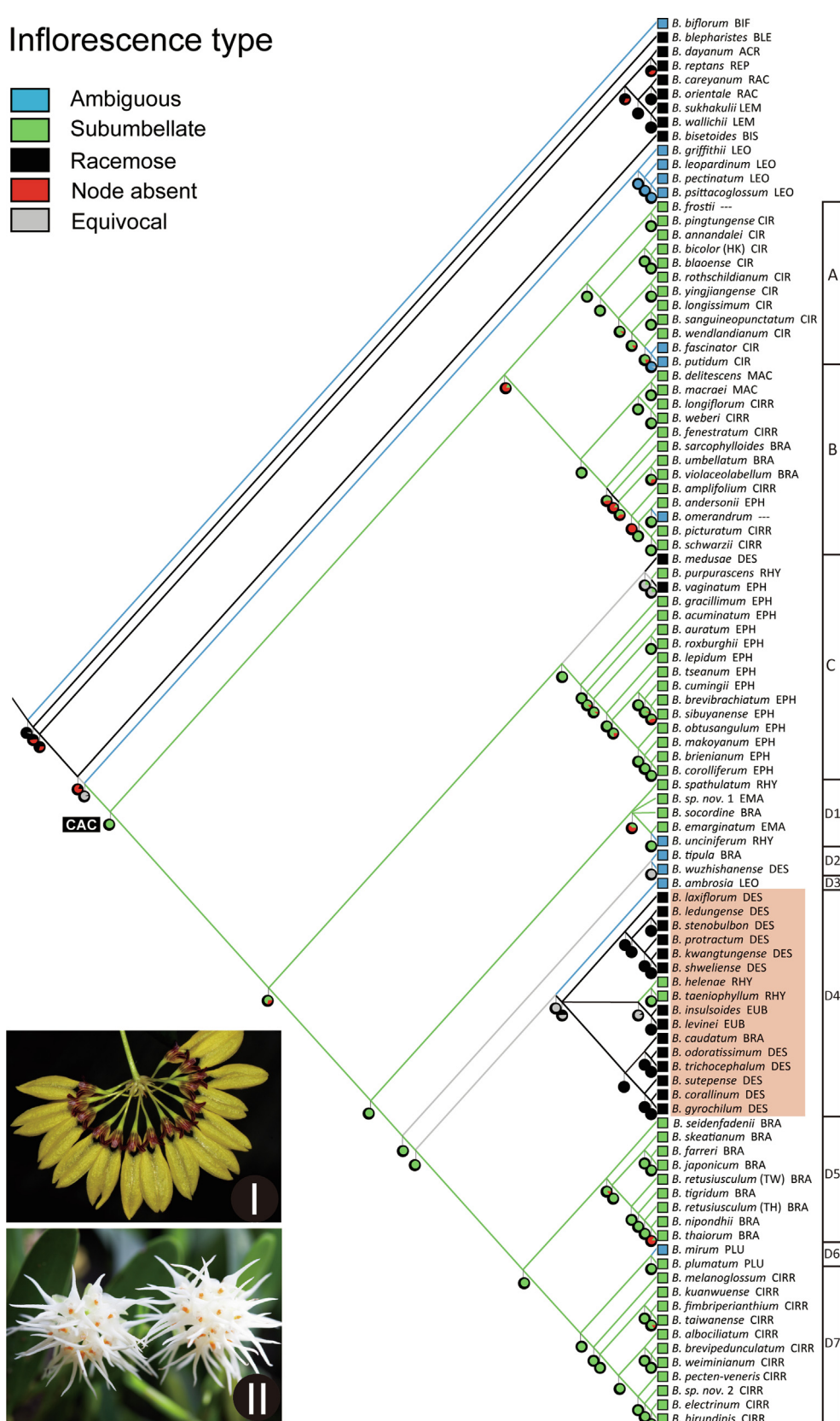


**Fig. 3.** Ancestral character reconstruction of inflorescence types. Branch color indicates parsimony optimization of ancestral character states. Pie charts at each node illustrate likelihood reconstructions and show the proportion of average likelihood. Inset photos show a typical subumbellate inflorescence in *Bulbophyllum skeantanum* (I) and a raceme in *B. odoratissimum* (II), with the shaded area indicating an evolutionary transition detected in subclade D4. Letters and numbers in the bar indicate major clades recognized within the *Cirrhopetalum* alliance clade (CAC).

## Lateral sepal shapes

- Basally twisted
- Not basally twisted
- Node absent
- Equivocal

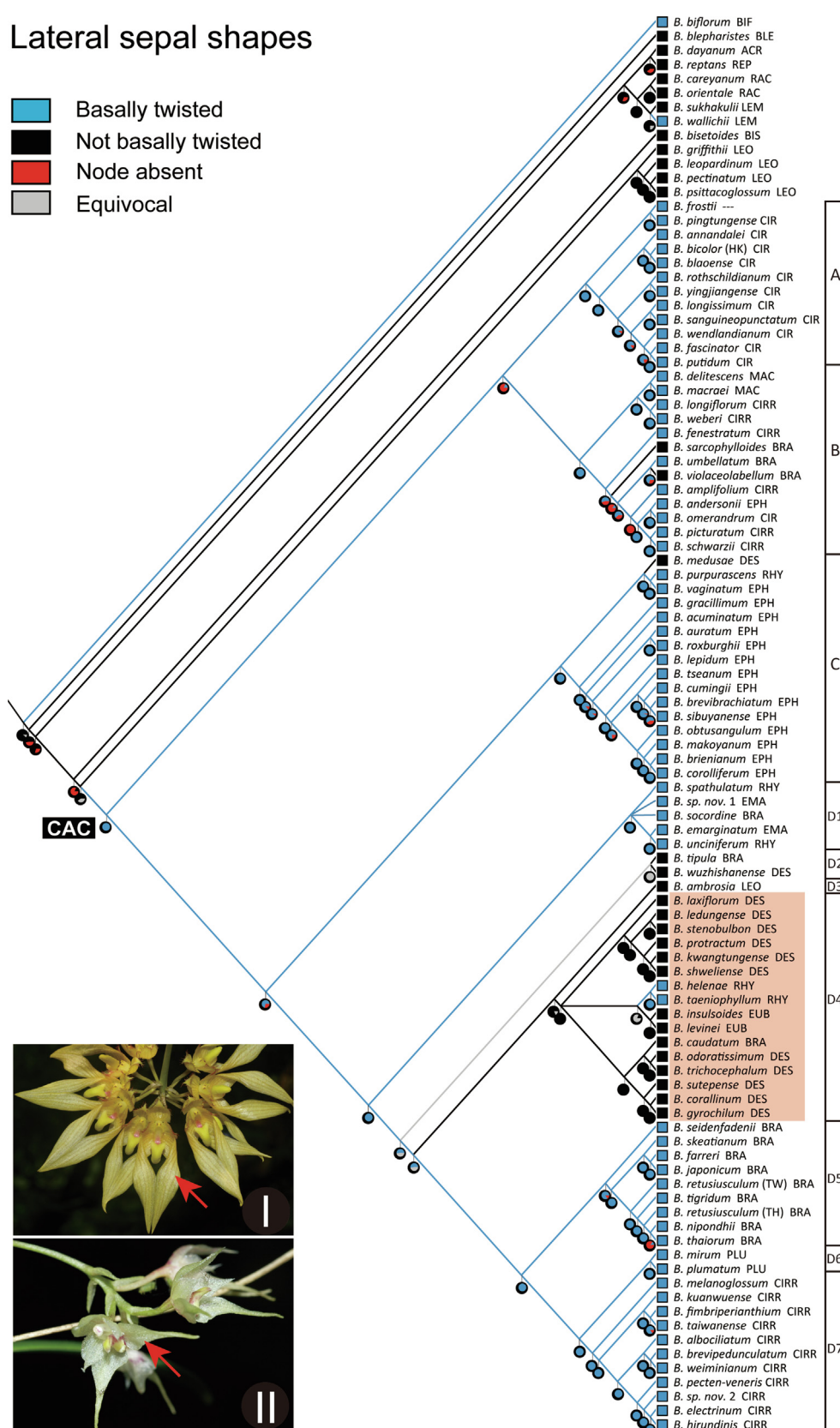


**Fig. 4.** Ancestral character reconstruction of lateral sepal shapes. Branch color indicates parsimony optimization of ancestral character states. Pie charts at each node illustrate likelihood reconstructions and show the proportion of average likelihood. Inset photos show basally twisted lateral sepals in *Bulbophyllum annandalei* (I) and straight lateral sepals in *B. levinei* (II), with the shaded area indicating an evolutionary transition detected in subclade D4. Letters and numbers in the bar indicate major clades recognized within the *Cirrhopetalum* alliance clade (CAC).

## Lateral sepal margin connation


 Upper margins connate  
 Lower margins connate  
 Free  
 Node absent  
 Equivocal

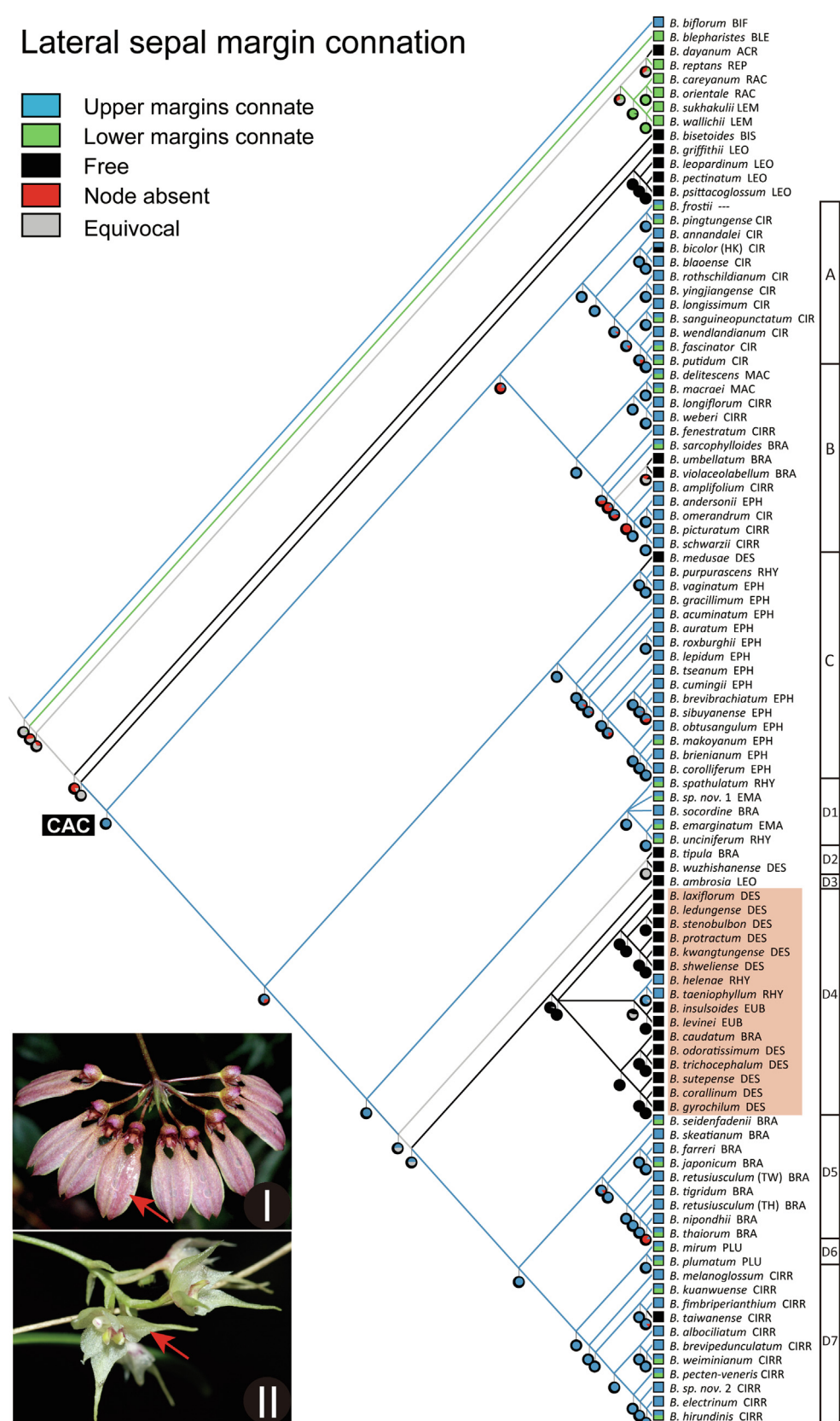


**Fig. 5.** Ancestral character reconstruction of lateral sepal margin connation. Branch color indicates parsimony optimization of ancestral character states. Pie charts at each node illustrate likelihood reconstructions and show the proportion of average likelihood. Inset photos show connate lateral sepals in *Bulbophyllum weberi* (I) and free lateral sepals in *B. levinei* (II), with the shaded area indicating an evolutionary transition detected in subclade D4. Letters and numbers in the bar indicate major clades recognized within the *Cirrhopetalum* alliance clade (CAC).

**Table 4**Estimation of Pagel's  $\lambda$  and Blomberg's K and the fit of different models of six continuously variable floral characters.

Character (absolute value)	Pagel's $\lambda$	K	Character (relative value)	Pagel's $\lambda$	K	Sig <sup>2</sup>	AICc/LnLik		pchisq		
							BM	OU	WH	OU ~ BM	OU ~ WH
DSL	0.94*/-	0.80*	log(DSL)	0.96*/-	0.92*	0.006	-62.27/33.21	-61.21/33.74	-4.68/4.41	> 0.05	< 0.05
DSW	0.93*/-	0.90*	log(DSW)	0.79*/△	0.83*	0.010	-16.75/10.45	-22.42/14.35	18.34/-7.10	< 0.05	< 0.05
LSL	0.72*/△	0.45*	log(LSL)	0.84*/△	0.65*	0.021	45.97/-19.84	46.77/-21.32	87.77/-41.82	> 0.05	< 0.05
LSW	0.97*/-	0.71*	log(LSW)	0.82*/△	0.79*	0.007	-42.90/23.52	-43.37/24.33	2.59/0.77	> 0.05	< 0.05
LL	0.84*/△	0.93*	log(LL)	0.84*/△	1.02*	0.007	-51.65/27.90	-54.31/31.30	14.76/-5.31	< 0.05	< 0.05
LW	0.96*/-	1.28*	log(LW)	0.84*/△	1.15*	0.008	-34.87/19.50	-37.48/22.38	24.30/-10.08	< 0.05	< 0.05

BM: Brownian motion model; OU: Ornstein-Uhlenbeck model; WH: White noise model. Sig<sup>2</sup>, the rate of character evolution under BM model. “\*” indicates  $\lambda$  or K is significantly different from 0 (P-value < 0.01); “△” indicates  $\lambda$  is significantly different from 1 (P-value < 0.01), while “-” is not significantly different from 1 (P-value > 0.05); pchisq < 0.05 indicates P-value associated with the difference in log likelihoods is significant and the OU model of evolution is favoured over BM or WH models, while pchisq > 0.05 indicates the BM model can't be rejected compared to the OU model.

#### 4.2. Extensive non-monophyly of the majority of existing sections

Four major clades (A–D) are recognized within the *Cirrhopetalum* alliance, with Clade D subdivided into seven subclades (D1–D7). Several of these clades or subclades broadly correspond with supraspecific taxa in previous classifications of the *Cirrhopetalum* alliance, although the majority of existing sections are not supported as monophyletic in the present phylogeny (Fig. 2). In many cases, existing sections are essentially monophyletic apart from the inclusion of a small number of outliers, with or without a corresponding set of synapomorphies. For example, the well-supported Clade A (PP = 1; BP = 87) primarily comprises species of sect. *Cirrhopetaloides* (the CIR group; Fig. 2), with *B. pingtungense* S.S.Ying & S.C.Chen from sect. *Cirrhopetalum* nested within it. Synapomorphies for this clade include flowers with floral scents that mimic decaying organic matter (Supplementary Fig. S5) and hairy dorsal sepal and petal margins (Supplementary Figs. S6 and S7). Another strongly supported clade, Clade C (PP = 1; BP = 100), primarily comprises species of sect. *Ephippium* (the EPH group; Fig. 2), but includes *B. medusae* from sect. *Desmosanthes*, *B. purpurascens* Teijsm. & Binn. from sect. *Rhytionanthos*, and *B. tseanum* (S.Y.Hu & Barreto) Z.H.Tsi from sect. *Cirrhopetaloides*. No clear synapomorphy is identified for Clade C, although a small labellum was proposed as diagnostic for sect. *Ephippium*, distinguishing it from species in other clades (e.g. Clade A: the CIR group; and Clade B: the CIRR I group) with which it shares basally twisted lateral sepals with connate upper margins. Notably, *B. medusae* exhibits a set of autapomorphies (e.g. the compressed racemose inflorescence, straight and free lateral sepal; Figs. 1L, 3–5), distinguishing it from typical members of the *Cirrhopetalum* alliance but revealing an affiliation with species of sect. *Desmosanthes*; this probably contributed to its exclusion from the alliance in previous classifications based solely on morphology (e.g. Garay et al., 1994; Vermeulen et al., 2015).

In other cases, however, the existing sectional classification is

obviously in need of major revision as reflected by the present phylogeny. For example, sect. *Cirrhopetalum* is clearly polyphyletic and is represented in two major clades, B and D7 (Fig. 2). Clade B, the CIRR I group, is highly heterogeneous, primarily comprising species of sect. *Cirrhopetalum*, but with species from sects. *Brachyantha*, *Cirrhopetaloides*, *Ephippium* and *Macrostylidia* nested within it. Given the heterogeneity of floral characters confirmed here among constituent members of this clade, it is not surprising that previous attempts to identify synapomorphies failed.

Clade D (PP = 0.99; BP = 78), which is subdivided into seven subclades (D1–D7), is remarkably heterogeneous, with species from at least eight previously circumscribed sections. Subclade D1 (the EMA group; PP = 1; BP = 99) comprises species from sects. *Brachyantha*, *Emarginatae* and *Rhytionanthos*. Subclade D2 (PP = 1; BP = 99) comprises *B. tipula* Aver. from sect. *Brachyantha* and *B. wuzhishanense* X.H.Jin from sect. *Desmosanthes*, with identifiable morphological synapomorphies (Figs. 3–5; Supplementary Fig. S3), viz. single-flowered inflorescences and lateral sepal upper margins that are basally straight and free (e.g. Fig. 1L), distinguishing it from the remaining members of Clade D. Subclade D3 comprises a single species, *B. ambrosia* from sect. *Leopardinae*, which is distantly related to other members of the section as sister to the entire CAC (Fig. 2). *Bulbophyllum ambrosia* has never previously been considered a member of the *Cirrhopetalum* alliance (Seidenfaden, 1973; Garay et al., 1994; Chen and Vermeulen, 2009), probably due to its striking morphological differences compared to typical *Cirrhopetalum*-allied species, viz. a single-flowered inflorescence, a basally well-developed sac-shaped column foot and a significantly enlarged labellum (Chen and Vermeulen, 2009). Subclade D6 (PP = 1; BP = 100) includes *B. mirum* J.J.Sm and *B. plumatum* Ames (the PLU group), but lacks clear morphological synapomorphies based on the floral characters assessed in the present study. Vermeulen et al. (2015) nevertheless noted that species of the PLU group exhibit a longitudinally grooved column face, distinguishing them from species

**Table 5**

Summary of parameters of PGLS based on log-transformed values with different models focusing on two characters (LSL and LW).

Model	Intercept	Slope	Lambda (ML) (95.0% CI)	Residual standard error (RSE)	Adjusted R <sup>2</sup>	F-statistic	P-value
LSL ~ DSL	0.71	0.72	0.74 (0.47, 0.91)	0.09 on 86 DF	0.18	20.19 on 1 and 86 DF	< 0.01
LSL ~ DSW	1.06	0.47	0.76 (0.49, 0.91)	0.10 on 86 DF	0.09	9.55 on 1 and 86 DF	< 0.01
LSL ~ LSW	1.05	0.48	0.75 (0.46, 0.90)	0.10 on 86 DF	0.07	7.62 on 1 and 86 DF	< 0.01
LSL ~ LL	1.04	0.54	0.74 (0.45, 0.90)	0.10 on 86 DF	0.09	9.37 on 1 and 86 DF	< 0.01
LSL ~ LW	1.25	0.35	0.79 (0.52, 0.93)	0.10 on 86 DF	0.03	4.02 on 1 and 86 DF	> 0.05
LSL ~ (DSL + DSW + LSW + LL + LW)	–	–	0.69 (0.37, 0.88)	0.09 on 82 DF	0.18	4.75 on 5 and 82 DF	< 0.01
LW ~ DSL	-0.07	0.42	0.81 (0.62, 0.92)	0.06 on 86 DF	0.16	18.07 on 1 and 86 DF	< 0.01
LW ~ DSW	-0.02	0.52	0.80 (0.57, 0.93)	0.06 on 86 DF	0.33	42.9 on 1 and 86 DF	< 0.01
LW ~ LSL	0.14	0.12	0.81 (0.62, 0.92)	0.06 on 86 DF	0.03	3.78 on 1 and 86 DF	> 0.05
LW ~ LSW	-0.10	0.66	0.53 (0.14, 0.80)	0.05 on 86 DF	0.39	55.23 on 1 and 86 DF	< 0.01
LW ~ LL	-0.17	0.80	0.37 (NA, 0.79)	0.04 on 86 DF	0.58	119.80 on 1 and 86 DF	< 0.01
LW ~ (DSL + DSW + LSL + LSW + LL)	–	–	0 (NA, 0.51)	0.03 on 82 DF	0.81	74.87 on 5 and 82 DF	< 0.01

of other sections that also have fused upper lateral sepal margins.

Subclade D4 (PP = 1; BP = 82) consists of a polytomy (Fig. 2): the EUB–RHY group, including species belonging to sects. *Eublepharon* and *Rhytionanthos*; and the DES group, comprising species from sect. *Desmosanthes*. The DES group is diagnosed by several synapomorphies: a compressed or elongated racemose inflorescence, with flowers in which the lateral sepals are free and do not differ significantly in shape and size from the dorsal sepal (Figs. 3–5). From a morphological perspective, the placement of sect. *Desmosanthes* within the *Cirrhopetalum* alliance is therefore unexpected since these diagnostic floral characters differ strikingly with the synapomorphies that characterize the latter (Figs. 3–5).

Subclade D5 (PP = 0.85; BP = 75) primarily consists of species from sect. *Brachyantha* (the BRA group). It possesses a suite of diagnostic traits, including: a subumbellate inflorescence with multiple flowers; entire and glabrous sepal and petal margins; and lateral sepals that are basally twisted with connate upper margins. Several outliers associated with this group, such as *B. umbellatum* Lindl. and *B. sarcophylloides* Garay et al. in Clade B, and *B. socordine* J.J.Verm. & Cootes in Subclade D1, exhibit similar character states, highlighting homoplasy in floral evolution.

In summary, most of the current sections within the *Cirrhopetalum* alliance are not supported as monophyletic. Ancestral character reconstruction nevertheless failed to identify clear synapomorphies for most well-supported clades/subclades corresponding to current sectional classification based on 17 selected characters. More putatively diagnostic taxonomic characters should be investigated to achieve a new sectional classification of the *Cirrhopetalum* alliance, among which sectional limits and diagnostic characters can be identified with confidence.

#### 4.3. Phylogenetic signal in lateral sepal and labellum traits

All sepal and labellum traits (absolute and log-transformed variables) demonstrate significant phylogenetic signal based on Pagel's  $\lambda$  and Blomberg's K statistics ( $P < 0.01$ , rejecting  $\lambda = 0$ ). Pure Brownian motion is rejected as an explanation for the occurrence of phylogenetic signal among five of the six continuously variable characters (based on log-transformed variables), with their  $\lambda$  values differing significantly from 1 ( $P < 0.01$ ). The intermediate values of  $\lambda$  retrieved for most of the studied traits indicate that alternative models should be considered to explain their evolution, rather than accepting the pure Brownian motion model (BM) (Kamilar and Cooper, 2013; and references therein), even though considerable phylogenetic signal was detected. Similarly, the White noise model (WH) was consistently rejected for all studied traits. In contrast, the Ornstein-Uhlenbeck model (OU) was found to fit the observed evolutionary patterns for three traits (DSW, LL, and LW; OU ~ BM:  $pchisq < 0.05$ ; Table 4), suggesting that the OU model provides the best explanation of hypothesized trends. All  $\alpha$  values retrieved under the OU model exceed zero, providing further evidence that non-Brownian behavior is a plausible explanation for the evolution of dorsal sepal (DSW) and labellum (LL and LW) traits. Although this effect may not be marked given the relatively small  $\alpha$  values ( $< 1$ ), the OU evolutionary model has several attractive biological features: applicability of an OU model has been interpreted as an indicator of processes such as phylogenetic niche conservatism, convergent evolution and stabilizing selection (e.g. Wiens et al., 2010; Christin et al., 2013; Ingram and Mahler, 2013).

The phylogenetic conservatism of the labellum as revealed under the OU model is also reflected by Blomberg's K values, which are consistently  $> 1$  for both LL and LW (based on relative values; Table 4). This indicates that close relatives are more similar than expected under the BM model of trait evolution (Kamilar and Cooper, 2013), probably reflecting the relatively invariable size of the labellum within the *Cirrhopetalum* alliance (and more broadly within the genus *Bulbophyllum* as a whole), in which the majority of species possess a pollinator trapping

mechanism. The mechanical fit of this adaptive feature (i.e. the match between floral presentation and the size and weight of the fly that triggers labellum movement) is considered the most important factor in achieving pollination (Ong and Tam, 2019). As such, the size of the labellum could be important for identifying specific functional pollination groups, which in turn could provide insights into evolutionary constraints placed on the development of new labellum phenotypes. This inference has previously been verified by studies in species of Clade A (sapromyiophily in *B. ornatissimum* (Rchb.f.) J.J.Sm.: Christensen, 1994; and *B. bicolor* Lindl.: Hu et al., 2017b), Clade C (non-rewarding fly pollination in sect. *Ephippium*: Ong and Tam, 2019) and *B. ambrosia* (honeybee pollination: Chen and Gao, 2011).

Conversely, the OU evolutionary model receives less support than the BM model in explaining the evolution of lateral sepal traits (LSL and LSW; OU ~ BM:  $pchisq > 0.05$ ; Table 4). Relatively low phylogenetic signal is inferred for LSL, with  $K < 1$  (Table 4), although this result is not corroborated by Pagel's  $\lambda$ . K values  $< 1$  indicate independence of trait evolution, suggesting that close relatives are less similar on average than more distant ones (Kamilar and Cooper, 2013). The labile evolutionary pattern observed for lateral sepals is reflected by an evolutionary trend in which the length of the sepal varies randomly across the phylogeny (results of mapping continuous characters not shown); a relatively higher rate of evolution ( $Sig^2 = 0.021$ ) is accordingly detected for LSL. The degree of variation observed in lateral sepal length is not explained by associated characters (the adjusted  $R^2$  ranges from 0.03 to 0.18; Table 5), suggesting that lateral sepal length evolves independently of other floral traits. Given this, it is plausible that a different suite of selective agents (i.e. pollinator-mediated selection) intervened during the evolution of lateral sepals in the *Cirrhopetalum* alliance.

Caution is nevertheless necessary when interpreting the OU model, since the link to stabilizing selection is not straightforward. The OU model is statistically complex and its properties are still poorly understood (Cooper et al., 2016). Any model of trait evolution (including the OU model) that attempts to account for non-Brownian behavior is susceptible to measurement error, which could confuse interpretation of evolutionary patterns. Many issues associated with misinterpretation of results can nevertheless be resolved by inspecting the  $\alpha$  parameter when the OU model is favored; simulation under the null model or Bayesian approaches for fitting models have also been recommended (Cooper et al., 2016). Attention should also be paid to the estimated value of Pagel's  $\lambda$  or Blomberg's K, since previous stimulation studies suggest that different evolutionary processes can give rise to similar phylogenetic signals and that similar processes can produce substantially different phylogenetic signal signatures, suggesting that its utility for inferring specific evolutionary histories may be limited (Hansen and Orzack, 2005; Diniz-Filho et al., 2012). The magnitude of  $\lambda$  or K may furthermore be affected by taxon sampling (Losos, 2008; Münkemüller et al., 2012). In particular, pseudo-chronograms can lead to strong over-estimation of phylogenetic signal reflected in K values, although  $\lambda$  appears to be unaffected by unresolved phylogenies (polymorphisms) and suboptimal branch-length information (Molina-Venegas and Rodríguez, 2017). Under such scenarios, Pagel's  $\lambda$  is suggested to be a more robust alternative to Blomberg's K for testing phylogenetic signal where phylogenetic information is incomplete. However, the constraint that  $\lambda$  cannot exceed 1 limits the utility of  $\lambda$  for identifying conditions that might increase phylogenetic signal over that expected under Brownian motion (Revell et al., 2008). Phylogenetic signal could therefore be interpreted appropriately when referring to both parameters alongside assessments of correlations among characters. In the present study, we detected phylogenetic signals that correspond with patterns of correlations among characters based on a robust phylogeny and utilizing several representative characters. Results from the best-fit model and rate of character evolution mirror the observed patterns to the extent that we are able to infer evolutionary trends in floral characters in relation to their function during pollination. These preliminary

results are of considerable value for future integrated studies that should make use of additional floral characters and a more comprehensive understanding of pollinator behavior.

## 5. Conclusions

Our phylogeny, based on four DNA regions and a far denser taxon sampling than previously achieved, provides a well-resolved phylogenetic framework for the *Cirrhopetalum* alliance, with the power to inform future taxonomic research as well as enable clarification of evolutionary transitions. The results of our phylogenetic analyses and ancestral character state reconstructions provide unequivocal evidence for the recognition of an amended *Cirrhopetalum* alliance as a well-supported monophyletic group, which is furthermore supported by a combination of synapomorphies—a subumbellate inflorescence and lateral sepals with upper margins that are basally twisted and mutually connate. The most striking result of the present study is that sect. *Desmosanthes* is confirmed as a member of the *Cirrhopetalum* alliance, revolutionizing our understanding of the alliance: ancestral character state reconstructions identify significant evolutionary transitions of floral characters exhibited in Subclade D4 (the DES group), with a set of synapomorphies that contrast with traits possessed by other members of the alliance. The existing sectional classification of the *Cirrhopetalum* alliance is shown to be highly artificial, with the majority of sections not supported as monophyletic. We advocate further targeted research to achieve better sampling within these sections in order to refine sectional boundaries and identify diagnostic characters before any formal nomenclatural changes are proposed. Previous circumscription of polyphyletic or paraphyletic taxa has undoubtedly hampered our understanding of the evolution of floral characters in the alliance. Significant evolutionary transitions of floral characters are here recognized among several clades within the *Cirrhopetalum* alliance for the first time.

Investigation of floral traits linked to functionally important floral organs (e.g. lateral sepals and labellum) in a phylogenetic context enables detection of contrasting phylogenetic signal (indicating traits that show phylogenetic conservatism or are evolutionarily labile) linked to different functional roles with regard to pollinator trapping. These preliminary results represent an ideal foundation for future comparative studies aimed at understanding the process of pollinator-mediated selection, and thus speciation and diversification within the *Cirrhopetalum* alliance. Integrated comparative phylogenetic approaches—particularly combining morphology, pollinator behavior, phylogenomics, physiology and ecology—should be applied to further unveil diversification in this species-rich group.

## Declaration of Competing Interest

The authors declare that the research was conducted in the absence of any commercial or financial relationships that could be construed as a potential conflict of interest.

## Acknowledgements

We thank D.P. Ye, J.W. Li, M.G. Agoo and J.R.C. Callado for assisting with fieldwork in China and the Philippines; B.M. Wang, L.V. Averyanov, J.J. Vermeulen, J.W. Zhai, L. Li, M.Z. Huang, O.P. Teck, R. Go, X.H. Jin and X.L. Zheng for providing materials and sharing literature; and F. Yang, G.Q. Zhang and X.Y. Wu for lab assistance. We are grateful for assistance from the Orchid Conservation Section at Kadoorie Farm and Botanic Garden (Hong Kong), National Orchid Conservation Centre (China), and Dr Cecilia Koo Botanic Conservation Center (Taiwan). We appreciate the constructive comments received from the anonymous reviewers, which greatly improved the manuscript.

## Funding

This work was supported by a doctoral research bursary to AQH from Kadoorie Farm & Botanic Garden.

## Appendix A. Supplementary material

Supplementary data to this article can be found online at <https://doi.org/10.1016/j.ympev.2019.106689>.

## References

- Averyanov, L.V., Nong, V.D., Nguyen, K.S., Maisak, T.V., Nguyen, V.C., Phan, Q.T., et al., 2016. New species of orchids (Orchidaceae) in the flora of Vietnam. *Taiwania* 61, 319–354.
- Barretto, G., Cribb, P., Gale, S., 2011. The Wild Orchids of Hong Kong. Natural History Publications (Borneo), Kota Kinabalu.
- Blomberg, S.P., Garland, T., 2002. Tempo and mode in evolution: phylogenetic inertia, adaptation and comparative methods. *J. Evol. Biol.* 15, 899–910.
- Blomberg, S.P., Garland, T., Ives, A.R., 2003. Testing for phylogenetic signal in comparative data: behavioral traits are more labile. *Evolution* 57, 717–745.
- Bouckaert, R., Heled, J., Kühnert, D., Vaughan, T., Wu, C.-H., Xie, D., Suchard, M.A., et al., 2014. BEAST 2: a software platform for Bayesian evolutionary analysis. *PLoS Comput. Biol.* 10, e1003537.
- Bradshaw, A.D., 1991. Genostasis and the limits to evolution. *Phil. Trans. R. Soc. B* 333, 289–305.
- Brown, J.M., Hettke, S.M., Lemmon, A.R., Lemmon, E.M., 2010. When trees grow too long: investigating the causes of highly inaccurate Bayesian branch-length estimates. *Syst. Biol.* 59, 145–161.
- Chase, M.W., Cameron, K.M., Freudenstein, J.V., Pridgeon, A.M., Salazar, G., van den Berg, C., et al., 2015. An updated classification of Orchidaceae. *Bot. J. Linn. Soc.* 177, 151–174.
- Chen, L.-L., Gao, J.-Y., 2011. Reproductive ecology of *Bulbophyllum ambrosia* (Orchidaceae). *Chin. J. Plant Ecol.* 35, 1202–1208.
- Chen, S.C., Vermeulen, J.J., 2009. *Bulbophyllum Thouars*. In: Wu, Z.Y., Raven, P.H., Hong, D.Y. (Eds.). Flora of China, vol. 25. Science Press and St. Louis: Missouri Botanical Garden Press, Beijing.
- Christensen, D.E., 1994. Fly pollination in the Orchidaceae. In: Arditti, J. (Ed.), *Orchid Biology: Reviews and Perspectives*, VI. Comstock, New York, pp. 415–454.
- Christin, P.A., Osborne, C.P., Chatelet, D.S., Columbus, J.T., Besnard, G., Hodgkinson, T.R., Garrison, L.M., et al., 2013. Anatomical enablers and the evolution of C<sub>4</sub> photosynthesis in grasses. *Proc. Natl. Acad. Sci.* 110, 1381–1386.
- Conran, J.G., Bannister, J.M., Lee, D.E., 2009. Earliest orchid macrofossils: Early Miocene *Dendrobium* and *Earina* (Orchidaceae: Epidendroideae) from New Zealand. *J. Bot.* 96, 466–474.
- Cooper, N., Thomas, G.H., Venditti, C., Meade, A., Freckleton, R.P., 2016. A cautionary note on the use of Ornstein-Uhlenbeck models in macroevolutionary studies. *Biol. J. Linn. Soc. Lond.* 118, 64–77.
- Darriba, D., Taboada, G.L., Doallo, R., Posada, D., 2012. jModelTest 2: more models, new heuristics and high-performance computing. *Nat. Methods* 9, 772.
- de Mazancourt, C., Johnson, E., Barracough, T.G., 2008. Biodiversity inhibits species' evolutionary responses to changing environments. *Ecol. Lett.* 11, 380–388.
- Diniz-Filho, J.A.F., Santos, T., Rangel, T.F., Bini, L.M., 2012. A comparison of metrics for estimating phylogenetic signal under alternative evolutionary models. *Genet. Mol. Biol.* 35, 673–679.
- Doyle, J.J., Doyle, J.L., 1987. A rapid DNA isolation procedure for small quantities of fresh leaf tissue. *Phytochem. Bull.* 19, 11–15.
- Felsenstein, J., 1973. Maximum likelihood estimation of evolutionary trees from continuous characters. *Am. J. Hum. Genet.* 25, 471–492.
- Fischer, G.A., Gravendeel, B., Sieder, A., Adriantiana, J., Heiselmayer, P., Cribb, P.J., et al., 2007. Evolution in resumption of Malagasy species of *Bulbophyllum* (Orchidaceae). *Molec. Phylogen. Evol.* 45, 358–376.
- Gamisch, A., Comes, H.P., 2019. Clade-age-dependent diversification under high species turnover shapes species richness disparities among tropical rainforest lineages of *Bulbophyllum* (Orchidaceae). *BMC Evol. Biol.* 19, 93.
- Gamisch, A., Fischer, G.A., Comes, H.P., 2015. Multiple independent origins of auto-pollination in tropical orchids (*Bulbophyllum*) in light of the hypothesis of selfing as an evolutionary dead end. *BMC Evol. Biol.* 15, 192.
- Garay, L.A., Hamer, F., Siegerist, E.S., 1994. The genus *Cirrhopetalum* and the genera of the *Bulbophyllum* alliance. *Nord. J. Bot.* 14, 609–646.
- Gravendeel, B., Fischer, G.A., Vermeulen, J.J., 2014. *Bulbophyllum Thouars*. In: Pridgeon, A.M., Cribb, P.J., Chase, M.W., Rasmussen, F.N. (Eds.), *Genera orchidacearum*, vol. 6. Oxford University Press, Oxford.
- Gravendeel, B., Smithson, A., Slik, F.J.W., Schuiteman, A., 2004. Epiphytism and pollinator specialization: Drivers for orchid diversity? *Phil. Trans. R. Soc. B* 359, 1523–1535.
- Hansen, T.F., 1997. Stabilizing selection and the comparative analysis of adaptation. *Evolution* 51, 1341–1351.
- Hansen, T.F., Orzack, S.H., 2005. Assessing current adaptation and phylogenetic inertia as explanations of trait evolution: the need for controlled comparisons. *Evolution* 59, 2063–2072.
- Harmon, L.J., Weir, J.T., Brock, C.D., Glor, R.E., Challenger, W., 2008. GEIGER:

- investigating evolutionary radiations. *Bioinformatics* 24, 129–131.
- Holtum, R. E., 1957. Orchids of Malaya. Flora of Malaya, vols. 1 & 2. Singapore.
- Holtum, R.E., 1964. A Revised Flora of Malaya. Government Printing Office, Singapore.
- Hosseini, S., Dadkhah, K., Go, R., 2016. Molecular systematics of genus *Bulbophyllum* (Orchidaceae) in Peninsular Malaysia based on combined nuclear and plastid DNA sequences. *Biochem. Syst. Ecol.* 65, 40–48.
- Hosseini, S., Go, R., Dadkhah, K., Nuruddin, A.A., 2012. Studies on maturase K sequences and systematic classification of *Bulbophyllum* in Peninsular Malaysia. *Pakistan J. Bot.* 44, 2047–2054.
- Hu, A.-Q., Gale, S.W., Kumar, P., Saunders, R.M.K., Sun, M., Fischer, G.A., 2017a. Preponderance of clonality triggers loss of sex in *Bulbophyllum bicolor*, an obligately outcrossing epiphytic orchid. *Molec. Ecol.* 26, 3358–3372.
- Hu, A.-Q., Ye, D.-P., Gale, S.W., Saunders, R.M.K., Fischer, G.A., Li, J.-W., 2017b. *Bulbophyllum jingdongense* (Orchidaceae), a new species in the *Cirrhopetalum* alliance from South China and Laos. *Phytotaxa* 307, 199–204.
- Huelsenbeck, J.P., Ronquist, F., 2001. MRBAYES: Bayesian inference of phylogenetic trees. *Bioinformatics* 17, 754–755.
- Ingram, T., Mahler, D.L., 2013. Surface: detecting convergent evolution from comparative data by fitting Ornstein-Uhlenbeck models with stepwise Akaike Information Criterion. *Methods Ecol. Evol.* 4, 416–425.
- Jersáková, J., Johnson, S.D., Kindlmann, P., 2006. Mechanisms and evolution of deceptive pollination in orchids. *Biol. Rev. Camb. Philos. Soc.* 81, 219–235.
- Kamilar, J.M., Cooper, N., 2013. Phylogenetic signal in primate behaviour, ecology and life history. *Phil. Trans. R. Soc. B* 368, 20120341.
- Katoh, K., Asimenos, G., Toh, H., 2009. Multiple alignment of DNA sequences with MAFFT. *Meth. Molec. Biol.* 537, 39–64.
- Kearse, M., Moir, R., Wilson, A., Stones-Havas, S., Cheung, M., Sturrock, S., et al., 2012. Geneious Basic: an integrated and extendable desktop software platform for the organization and analysis of sequence data. *Bioinformatics* 28, 1647–1649.
- Lewis, P.O., 2001. A likelihood approach to estimating phylogeny from discrete morphological character data. *Syst. Biol.* 50, 913–925.
- Losos, J.B., 2008. Phylogenetic niche conservatism, phylogenetic signal and the relationship between phylogenetic relatedness and ecological similarity among species. *Ecol. Lett.* 11, 995–1007.
- Maddison, W. P., Maddison, D. R., 2011. Mesquite: A modular system for evolutionary analysis, version 2.7.5. Available at: <http://mesquiteproject.org>.
- Marshall, D.C., 2010. Cryptic failure of partitioned Bayesian phylogenetic analyses: lost in the land of long trees. *Syst. Biol.* 59, 108–117.
- Martins, E.P., Hansen, T.F., 1997. Phylogenies and the comparative method: a general approach to incorporating phylogenetic information into the analysis of interspecific data. *Am. Nat.* 149, 646–667.
- Miller, M.A., Pfeiffer, W., Schwartz, T., 2010. Creating the CIPRES Science Gateway for inference of large phylogenetic trees. Paper presented at Proceedings of the Gateway Computing Environments Workshop (GCE).
- Molina-Venegas, R., Rodríguez, M.Á., 2017. Revisiting phylogenetic signal: strong or negligible impacts of polytomies and branch length information? *BMC Evol. Biol.* 17, 53.
- Münkemüller, T., Lavergne, S., Bzeznik, B., Dray, S., Jombart, T., Schiffrers, K., Thuiller, W., 2012. How to measure and test phylogenetic signal. *Method Ecol. Evol.* 3, 743–756.
- Nylander, J.A., Wilgenbusch, J.C., Warren, D.L., Swofford, D.L., 2008. AWTY (are we there yet?): a system for graphical exploration of MCMC convergence in Bayesian phylogenetics. *Bioinformatics* 24, 581–583.
- Ong, P.T., Tam, S.M., 2019. Pollination notes for seven *Bulbophyllum* species (Section *Ephippium*) from Peninsular Malaysia. *Malesian Orchid J.* 23, 87–96.
- Orme, D., Freckleton, R., Thomas, G., Petzoldt, T., Fritz, S., Isaac, N., Pearse, W., 2013. Caper: comparative analyses of phylogenetics and evolution in R. R package version 0.4. Available from <http://CRAN.R-project.org/package=caper>.
- Pagel, M., 1997. Inferring evolutionary processes from phylogenies. *Zool. Scripta* 26, 331–348.
- Pagel, M., 1999. Inferring the historical patterns of biological evolution. *Nature* 401, 877–884.
- Pridgeon, A.M., Cribb, P.J., Chase, M.W., Rasmussen, F.N., 2014. Genera Orchidacearum Vol. 6 Oxford University Press, Oxford.
- Rambaut, A., 2014. FigTree v1.4.2, A Graphical Viewer of Phylogenetic Trees. Available from <http://tree.bio.ed.ac.uk/software/figtree/>.
- Rambaut, A., Drummond, A.J., 2014. LogCombiner v 2.1.3. Institute of Evolutionary Biology. University of Edinburgh, UK.
- Rambaut, A., Suchard, M. A., Xie, D., Drummond, A. J., 2014. Tracer v.1.6, available from <http://beast.bio.ed.ac.uk/Tracer>.
- Revell, L.J., 2012. phytools: an R package for phylogenetic comparative biology (and other things). *Methods Ecol. Evol.* 3, 217–223.
- Revell, L.J., Harmon, L.J., Collar, D.C., 2008. Phylogenetic signal, evolutionary process, and rate. *Syst. Biol.* 57, 591–601.
- Scopece, G., Cozzolino, S., Johnson, S.D., Schiestl, F.P., 2010. Pollination efficiency and the evolution of specialized deceptive pollination systems. *Am. Nat.* 175, 98–105.
- Seidenfaden, G., 1973. Notes on *Cirrhopetalum* Lindl. *Dansk Bot. Arkiv.* 29, 1–260.
- Seidenfaden, G., 1979. Orchid genera in Thailand VIII: *Bulbophyllum* Thou. *Dansk Bot. Arkiv.* 33, 1–228.
- Seidenfaden, G., Wood, J.J., 1992. The Orchids of Peninsular Malaysia and Singapore. Olsen & Olsen, Fredensborg.
- Smidt, E.C., Borba, E.L., Gravendeel, B., Fischer, G.A., van den Berg, C., 2011. Molecular phylogeny of the Neotropical sections of *Bulbophyllum* (Orchidaceae) using nuclear and plastid spacers. *Taxon* 60, 1050–1064.
- Stamatakis, A., 2014. RAxML version 8: a tool for phylogenetic analysis and post-analysis of large phylogenies. *Bioinformatics* 30, 1312–71313.
- Thouars, L., 1822. Histoire particulière des plantes orchidées recueillies sur les trois îles australes d'Afrique, de France, de Bourbon et de Madagascar, t. 3.
- van der Cingel, N.A., 2001. An atlas of orchid pollination: America, Africa, Asia and Australia. A.A Balkema, Rotterdam.
- Vermeulen, J.J., 2014. Asian sections of *Bulbophyllum* Thouars. In: In: Pridgeon, A.M., Cribb, P.J., Chase, M.W., Rasmussen, F.N. (Eds.), Genera Orchidacearum, vol. 6. Oxford University Press, Oxford, pp. 19–40.
- Vermeulen, J.J., Coates, J., 2008. Two new species of *Bulbophyllum* from the Philippines. *Males. Orchid J.* 1, 147–151.
- Vermeulen, J. J., O'Byrne, P., Lamb A., 2015. *Bulbophyllum* of Borneo. National History Publications (Borneo), Kota Kinabalu.
- Vermeulen, J.J., Schuiteman, A., de Vogel, E.F., 2014. Nomenclatural changes in *Bulbophyllum* (Orchidaceae; Epidendroideae). *Phytotaxa* 166, 101–113.
- Wang, J.Y., Liu, Z.J., Wu, X.Y., Huang, J.X., 2017. *Bulbophyllum lipingtaoi*, a new orchid species from China: evidence from morphological and DNA analyses. *Phytotaxa* 295, 218–226.
- Wiens, J.J., Ackerly, S.D., Allen, A.P., Anacker, B.L., Buckley, L.B., Cornell, H.V., et al., 2010. Niche conservatism as an emerging principle in ecology and conservation biology. *Ecol. Lett.* 13, 1310–1324.
- Xiang, X.G., Schuiteman, A., Li, D.Z., Huang, W.C., Chung, S.W., Li, J.W., et al., 2013. Molecular systematics of *Dendrobium* (Orchidaceae, Dendrobieae) from mainland Asia based on plastid and nuclear sequences. *Molec. Phylogen. Evol.* 69, 950–960.
- Zhai, J., Chen, X., Chen, Y., Wang, B., 2017. *Bulbophyllum yingjiangense*, a new species from Yunnan, China: morphological and molecular evidence (Orchidaceae; Epidendroideae). *Phytotaxa* 298, 77–82.
- Zhang, C., Rannala, B., Yang, Z., 2012. Robustness of compound Dirichlet priors for Bayesian inference of branch lengths. *Syst. Biol.* 61, 779–784.